

Re-rank Coarse Classification with Local Region Enhanced Features for Fine-Grained Image Recognition

Shaokang Yang*, Shuai Liu†, Cheng Yang, Changhu Wang

ByteDance AI Lab, Beijing, China

{yangsk0205, sliu012}@gmail.com, {yangcheng.iron, wangchanghu}@bytedance.com

Abstract

Fine-grained image recognition is very challenging due to the difficulty of capturing both semantic global features and discriminative local features. Meanwhile, these two features are not easy to be integrated, which are even conflicting when used simultaneously. In this paper, a retrieval-based coarse-to-fine framework is proposed, where we re-rank the TopN classification results by using the local region enhanced embedding features to improve the Top1 accuracy (based on the observation that the correct category usually resides in TopN results). To obtain the discriminative regions for distinguishing the fine-grained images, we introduce a weakly-supervised method to train a box generating branch with only image-level labels. In addition, to learn more effective semantic global features, we design a multi-level loss over an automatically constructed hierarchical category structure. Experimental results show that our method achieves state-of-the-art performance on three benchmarks: CUB-200-2011, Stanford Cars and FGVC Aircraft. Also, visualizations and analysis are provided for better understanding.

1. Introduction

Fine-grained visual classification (FGVC) aims at recognizing subordinate categories that belong to the same superior class, such as distinguishing different kinds of wild birds[33], cars[19] or airs[26]. Unlike general classification tasks, fine-grained sub-categories usually have similar appearances, which can only be classified by some subtle details. For instance, the difference between *Yellow Throated Vireo* and *White Eyed Vireo* is the color of certain parts as shown in Fig 1 (a).

To address this task, lots of methods were proposed that

*Corresponding author (equal contribution)

†Corresponding author (equal contribution)

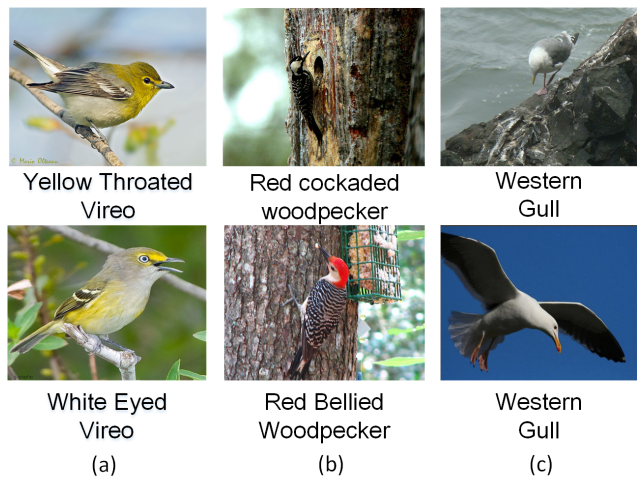


Figure 1. Some hard instances from the CUB-200-2011[33]. Sub-figure (a) and (b) show very similar categories, where the subtle differences lie in the color of certain parts. Sub-figure (c) shows the different poses of the same category.

can be divided into global-based methods[21, 7, 30] and part/attention-based methods[38, 12, 16, 9, 20, 47]. Most of them aim at learning more effective global/part features separately and adopt a softmax to predict final classification results. Unlike these methods, in this work, we propose a novel retrieval-based model that can simultaneously learn effective global features and discriminative local features inspired by DELG[4]. We refer to the new model as Coarse Classification and Fine Re-ranking (CCFR), where local region enhanced features are generated to re-rank the classification results predicted by the conventional global pooling features. Specifically, our model includes two main branches. One targets to select *topn* classification results (named as Coarse Classification) predicted by global features, the other aims at learning discriminative local-region features that are fused with global features to build a search-

ing database for re-ranking the Coarse Classification results. By this way, our CCFR can make use of the local region enhanced features to correct images which cannot be distinguished accurately only relying on global features. For instance, merely depending on global features failed when the object scale is too small in a full image or the subtle difference lies in some local regions as shown in Fig 1.

Therefore, the key to our model is how to accurately localize the discriminative part regions. Recently, a number of methods[2, 3, 5, 11, 25, 37, 40] that utilized the object/part annotations (e.g. bird parts annotation in bird fine-grained classification) were proposed to accurately localize part regions. However, obtaining object/part annotations is very expensive. In this work, we propose a weakly-supervised method to effectively localize discriminative part regions with only image-level labels. Specifically, we leverage a Feature Pyramid Network (FPN)[24] to generate a series of multi-scale regions, where triplet loss[28] is used to make local regions more discriminative other than informative with ranking loss[38]. It is reasonable that discriminative local regions (e.g., bird’s head, bird’s wings) are more important for the FGVC task than the whole object regions containing the highest informativeness. Visualizations are provided in section 4.5. In addition, to learn more effective global semantic features, we utilize an unsupervised method to automatically construct a hierarchical category structure and then design a Multi-level loss to train our model. Overall, the main contributions of our work are listed as follows:

- We build a Coarse Classification and Fine Re-ranking(CCFR) architecture that simultaneously uses both global and part features by re-ranking.
- We propose a weakly-supervised method to effectively select discriminative local regions without object/part annotations.
- We utilize an unsupervised method to automatically construct a hierarchical category structure to learn more effective global semantic features.

2. Related Works

Fine-grained image classification aims at recognizing the objects of the sub-categories from visually similar category and has been studied for many years. Existing methods can be roughly categorized into two types: global-based methods[21, 7, 30] and part/attention-based methods[22, 41, 38, 12, 16, 9, 20, 47]. The former focuses on how to extract more effective pre-training parameters and design more useful pooling techniques. The latter targets at training a detection network for localizing part regions which are used to perform classification.

2.1. Global-based methods for FGVC

Cui et al.[7] utilizes large-scale datasets (e.g., ImageNet[8] and Inaturalist[32]) to learn more effective pre-training parameters for domain-specific FGVC tasks. To resolve the difference between these pre-training datasets and the target fine-grained datasets, they propose a measure to estimate domain similarity via Earth Mover’s Distance. And then they pre-selects certain classes from the large-scale datasets which match best to the current fine-grained datasets. Similarly, Krause et al.[18] collect images from the Internet to enrich the FGVC datasets proving the effectiveness of large-scale datasets for FGVC performance. Other methods aim at developing advanced pooling strategies. For instance, Lin et al.[23] propose a bilinear structure to compute the pairwise feature interactions by two independent CNN. Similar works are [29, 30, 45]. Besides, researchers also combine Fisher vectors to enhance the global representations [17, 43]. All of these works target at enriching the global features representation to obtain better classification results. In our model, to learn more effective global semantic features, we propose a Multi-level loss which depends on an automatically constructed hierarchical category structure.

2.2. Part-based methods for FGVC

One can design a part-based classification method by employing the part annotations if they exist. However, such annotations are expensive and usually unavailable, and the current researchers mainly focus on localizing part-region with only image-level labels[1, 15, 31, 27, 46, 42, 35]. He et al.[13] propose a sophisticated reinforcement learning method to estimate how many and which image regions are helpful to distinguish the categories. Ge et al.[12] use Mask R-CNN and CRF-based segmentation alternately to extract rough object instances. However, such a multi-stage training process is hard to implement which significantly hamper the availability in practical use. Yang et al.[38] adopt a ranking loss to train an FPN network to obtain the most informative regions. However, such a loss function encourages the model to select boxes containing entire objects other than discriminative local regions. To overcome such a problem, we utilize the triplet loss to select more discriminative regions.

Cao et al.[4] design a DELG model that unifies global and local features into a single deep model to obtain accurate retrieval results on Image Retrieval Tasks. Inspired by this work, in our method we design a re-ranking policy to improve the performance by correcting the uncertain *topn* classification results.

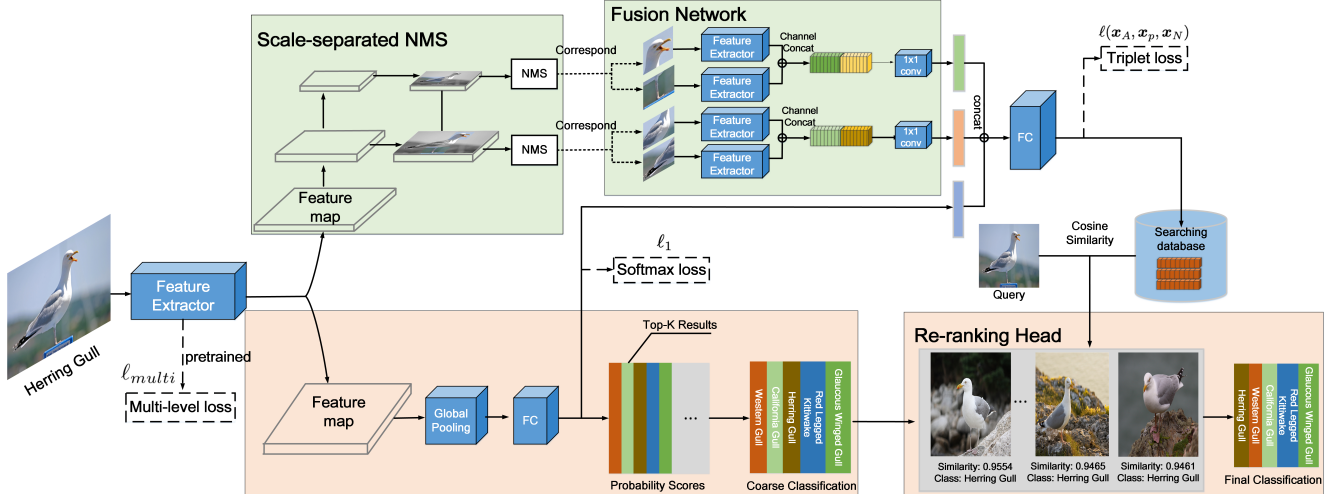


Figure 2. The overview of our CCFR architecture. It mainly includes two branches: 1) On the top branch, we utilize the Triplet loss and the Scale-separated NMS to discover more discriminative local regions, and integrate these region features with the whole image features to obtain the final embedding features, which are used to build a searching database. 2) On the bottom branch, we first obtain the Coarse Classifications (the *topn* Softmax probabilities), and then re-rank them by the statistic of the retrievals from the searching database. The Feature Extractor is pretrained by a proposed Multi-level loss and is updated by the combination of a Triplet loss and a Softmax loss during training.

3. Method

In this section, we describe our Coarse Classification and Fine Re-ranking (CCFR) architecture in detail. The overview is shown in Fig 2, which includes two main branches: 1) The top branch first extracts discriminative local-region features used to enhance global features, and then builds a database for re-ranking. 2) The bottom branch first acquires the *topn* classification results with global features, and then re-ranks them with the constructed searching database to obtain the final results. As shown in [21, 7, 30], satisfactory results were obtained based on global features, however, these methods usually fail in some cases depending on subtle parts (e.g., Fig 1). To solve such problems, a series of methods [38, 12, 16, 9, 20, 47] have been proposed to learn local features. However most of them only adopt the convention softmax classification. Unlike these methods, our CCFR is a retrieval-based method which can effectively correct the misclassified images with the combination of the *topn* classification and searching results. Besides, comparing with the current state-of-the-art StackLSTM [12] which is a very messy multi-stage training model, the model in our method is easier to implement and train.

3.1. Multi-level loss for learning effective global features

As we have known, feature expression is fundamental for visual classification tasks. How to learn effective features is the key to these tasks. The human visual cognition system

processes from rough to fine-grained. (e.g., we first realize that it belongs to a bird at a glance, and then we confirm that it belongs to *Vireo* or other bird types through careful observation.) To imitate the above cognition process, we organize the categories into Multi-level loss according to the visual appearance. Specifically, we first automatically construct a hierarchical category system through visual feature clustering. As shown in the Fig 3, the four birds on the top (bottom) are more similar to each other which can be naturally grouped into one super class. We then propose a Multi-level loss to utilize the constructed category system. We adopt two standard Softmax loss on the children (origin) category and super (cluster) category and then design a constraint loss between these two categories:

$$\ell_1 = - \sum_{i=1}^C \mathbf{y}_i \log \mathbf{p}_i \quad (1)$$

$$\ell_2 = - \sum_{j=1}^{C_f} \mathbf{y}_j \log \mathbf{p}_j \quad (2)$$

$$\ell_h = \max(0, \mathbf{p}_{children} - \mathbf{p}_{parent}) \quad (3)$$

where \mathbf{p}_i is the probability of class i in children categories, \mathbf{p}_j is the probability of class j in super categories, $\mathbf{p}_{children}$ denotes the average of all children category probabilities belonging to the same super category, and \mathbf{p}_{parent} is the corresponding super category probability, C is the number of children classes, C_f is the number of super classes, and ℓ_1 and ℓ_2 are the standard Softmax loss. ℓ_h is

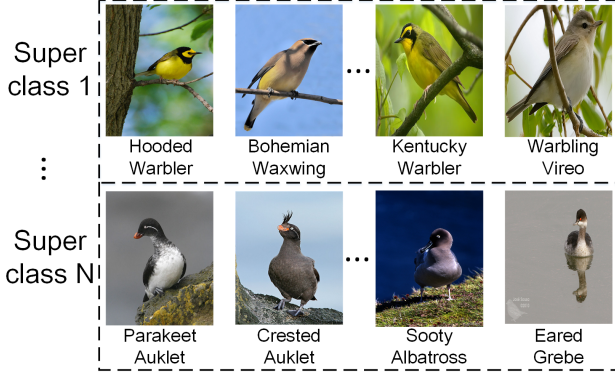


Figure 3. The generated hierarchical categories by clustering. Birds with similar appearances are grouped into the same super class.

the constraint loss between super category probability and children’s. The final Multi-level loss is defined as follows:

$$\ell_{multi} = \ell_1 + \lambda * \ell_2 + \ell_h \quad (4)$$

where λ is the hyper-parameter. In our setting, $\lambda = 1$.

3.2. Localizing discriminative local regions with weakly supervising

To select discriminative local regions, we leverage a top-down pathway with lateral connections detection network inspired by the Feature Pyramid Networks (FPN)[24] as shown in Fig 2. We can obtain a series of feature maps with different spatial resolutions. By using these multi-scale feature maps, we can generate local regions among different scales and ratios. Specifically, for an input image of size 448, we set the bounding-box scales to $\{96, 192\}$ and aspect ratio to 1:1. Given that different parts of the object own different scales (e.g., the bird’s head area is smaller than its wings), performing NMS over boxes of all scales may result in larger boxes suppressing the smaller ones. Thus, we perform NMS on each scale separately (named as Scale-separated NMS). Then we resize the selected boxes to the pre-defined size (e.g., 224×224) and feed them into the feature extractor to obtain local features. To prevent overfitting, we share parameters of feature extractor used in local regions with the one used in global features. To better capture the spatial relationships among the different regions, for each scale, we concatenate the local features along the channel direction and fuse them with 1×1 convolution filters as shown in Fig 2 (we name it as Fusion Network).

The key of this process is how to select discriminative local regions. Given that the part/object annotations for FGVC are expensive, it is desirable to train the model with only image-level labels (weakly supervised). As mentioned above, the NTS utilized a ranking loss to select informative regions, other than discriminative regions, leading to

a preference for larger boxes (as shown in the top row of Fig 4). Triplet loss[28] has shown beneficial for learning discriminative local features by maximizing distance of different classes and minimizing the distance of the same class. Thus, we adopt the triplet loss to learn discriminative local features, which can be defined as follows:

$$\ell(\mathbf{x}_A, \mathbf{x}_p, \mathbf{x}_N) = \mathbf{f}(sim(\mathbf{x}_A, \mathbf{x}_p) - sim(\mathbf{x}_A, \mathbf{x}_N) - \mathbf{a}) \quad (5)$$

where $sim(\cdot)$ denotes the cosine similarity, \mathbf{x}_A is an anchor input, \mathbf{x}_p denotes a positive input of the same class as \mathbf{x}_A , \mathbf{x}_N is a negative input of a different class from \mathbf{x}_A , \mathbf{a} is a margin between positive and negative pairs, $\mathbf{f}(\cdot)$ is defined as follows:

$$\mathbf{f}(y) = max(0, -y) \quad (6)$$

where y is the value of $sim(\mathbf{x}_A, \mathbf{x}_p) - sim(\mathbf{x}_A, \mathbf{x}_N) - \mathbf{a}$. Each of (\mathbf{x}_A) , (\mathbf{x}_p) and (\mathbf{x}_N) is the embedding features by concatenating the fused local features and global features. Finally, the total loss is defined as:

$$\ell = - \sum_{i=1}^C \mathbf{y}_i \log \mathbf{p}_i + \mu * \ell(\mathbf{x}_A^i, \mathbf{x}_P^i, \mathbf{x}_N^i) \quad (7)$$

where μ is the hyper-parameter, in our setting $\mu = 1$.

3.3. Re-rank the coarse classification by retrieval

Up to now, we have obtained the *topn* probability scores (coarse classification results) and discriminative local enhanced features (anchor \mathbf{x}_A features). Then we construct the searching database using these features extracted from the training samples. We treat the image that needs to be reorganized as a query (\mathbf{q}), and by computing the cosine similarity between the query and the searching database we obtain the *topm* similarity scores with their labels. We finally re-rank the classification results based on these similarity scores and labels.

The detailed re-ranking formulation is listed as follows. Let $\mathbf{X} = \{\mathbf{x}_k^c\}$ be the selected training samples as the searching database, where \mathbf{x}_k^c is the local enhanced feature vector influenced by our model ($k = 1, 2, \dots, N$ is the sample index, $c = 1, 2, \dots, C$ is the class label index). Again, let $sim(\mathbf{q}, \mathbf{X}) = \{sim(\mathbf{q}, \mathbf{x}_k^c)\}$ be the similarity of the testing sample \mathbf{q} between all the training samples in the database. $rank(\mathbf{q}, \mathbf{X}, topm)$ is the most similar *topm* training samples of testing \mathbf{q} measured by $sim(\mathbf{q}, \mathbf{X})$

Then the finally re-ranked score of the testing sample \mathbf{q} w.r.t class c is

$$S_q^c = \begin{cases} S_f(\mathbf{q}, c), S_f(\mathbf{q}, c) \geq T_{sf} \\ \alpha * S_f(\mathbf{q}, c) + \beta * Sc(\mathbf{q}, c), S_f(\mathbf{q}, c) < T_{sf} \end{cases} \quad (8)$$

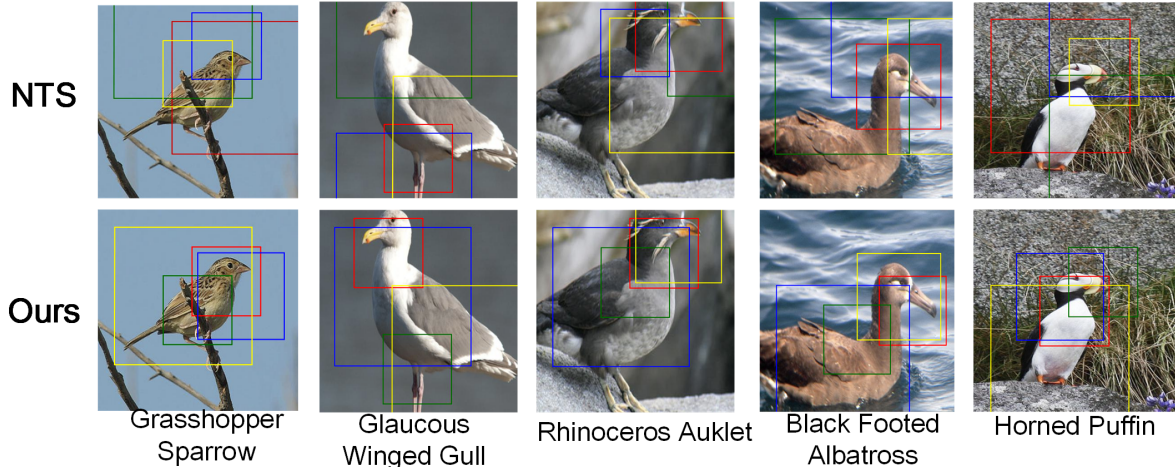


Figure 4. The Top4 selected boxes by NTS and our CCFR. Compared to NTS (the top row), our model tends to focus on smaller boxes containing discriminative parts.

Datasets	Train	Test	Category
CUB-200-2011	5,994	5,794	200
FGVC Aircraft	6,667	3,333	100
Stanford Cars	8,144	8,041	196

Table 1. Statistics of three datasets.

where α and β are the weights balancing the two terms, $S_f(\mathbf{q}, c)$ is the Softmax probability of \mathbf{q} w.r.t class c , T_{sf} is a threshold for softmax score, and $S_c(\mathbf{q}, c)$ is the normalized similarity score between query and the class c which is calculated as

$$S_c(\mathbf{q}, c) = \frac{\sum_{k=1}^{N_c} sim(\mathbf{q}, \mathbf{x}_k^c)}{\sum_{c=1}^{topn} \sum_{k=1}^{N_c} sim(\mathbf{q}, \mathbf{x}_k^c)} \quad (9)$$

s.t. $sim(\mathbf{q}, \mathbf{x}_k^c) > T_{sc}, \mathbf{x}_k^c \in rank(\mathbf{q}, \mathbf{X}, topn)$

where T_{sc} is a threshold score for searching similarity. In this way, we could probably distinguish and correct the extremely similar sub-categories which usually reside in the *topn* classification results with non-dominant softmax scores.

4. Experiments & Analysis

4.1. Datasets

We conduct comprehensive experiments to evaluate our proposed CCFR algorithm on Caltech-UCSD Birds (CUB-200-2011[33]), FGVC Aircraft[26] and Stanford Cars[19] which are popular benchmarks for fine-grained category classification. The details of these three datasets are shown in Table 1. Note that we only use the image-level labels in our all experiments.

Caltech-UCSD Birds. CUB-200-2011 is the most widely used dataset with 200 wild bird species. It contains 11,788 images spanning 200 sub-categories. The ratio of train data and test data is roughly 1:1 and each species has only 30 images for training.

FGVC Aircraft. FGVC Aircraft dataset consists of 10,000 images with 100 categories. The ratio of train data and test data is roughly 2:1. The dataset is organized in a four-level hierarchy, from finer to coarser: Model, Variant, Family, Manufacturer. Most images are airplanes.

Stanford Cars. Stanford Cars dataset consists of 16,185 images over 196 categories. The data is divided into 8,144 training images and 8,041 testing images, and each category has been divided roughly into a 50-50 split. Categories are typically at the level of Make, Model, Year (e.g. 2012 BMW M3 coupe).

4.2. Implementation Details

In all our implementations, ResNet-50 is chosen as the feature feature extractor. We preprocess each image to size 448×448 , and select 2 local regions for each scale (there are two scales), and set the NMS threshold to 0.25. We adopt Momentum SGD with an initial learning rate 0.001 and multiply it by 0.1 for each 30 epochs, and set the weight decay to $1e-4$, and set the batch-size to 16. We first utilize the ranking loss[38] to train the FPN for satisfactory detection performance, and then use the Softmax loss and Triplet loss to train our model. For re-ranking in Equation 8, we set the *topn* as 5, and set α to 0 and β to 1.0 which means only using the searching similarity when the Softmax probability is low. The threshold T_{sf} is set differently according to the roughly average Top1 Softmax probabilities on different datasets (here we set 0.5 on CUB-200-2011, and 0.7 on Cars

Method	Base Model	CUB Acc.(%)	Airs Acc.(%)	Cars Acc.(%)
ResNet-50[21]	ResNet-50	84.5	-	-
Spatial-RNN[36]	M-Net/D-Net	-	88.4	-
BCN[10]	ResNet-50	87.7	90.3	94.3
ACNet[14]	ResNet-50	88.1	92.4	94.6
DCL[6]	ResNet-50	87.8	93.0	94.5
DF-GMM[35]	ResNet-50	88.8	93.8	94.8
a-pooling[30]	ResNet-50	86.5	-	91.6
MA-CNN[44]	VGG-19	86.5	89.9	-
NTS[38]	ResNet-50	87.5	91.4	93.9
API-net[47]	ResNet-50	87.7	93.0	94.8
GCL[34]	ResNet-50	88.3	93.2	94.0
MGE[39]	ResNet-50	88.5	-	93.9
CS-Parts[16]	ResNet-50	89.5	-	92.5
Inceptin-v3[7]	Inception-v3	89.6	90.7	93.5
PMG[9]	ResNet-50	89.6	93.4	95.1
Mix+[20]	ResNet-50	90.2	92.0	94.9
StackedLSTM[12]	GoogleNet	90.4	-	-
Our CCFR w\o re-ranking	ResNet-50	90.7	93.0	95.37
Our CCFR	ResNet-50	91.1	94.1	95.49

Table 2. Comparison of different methods on CUB-200-0211, FGVC Aircraft and Stanford Cars.

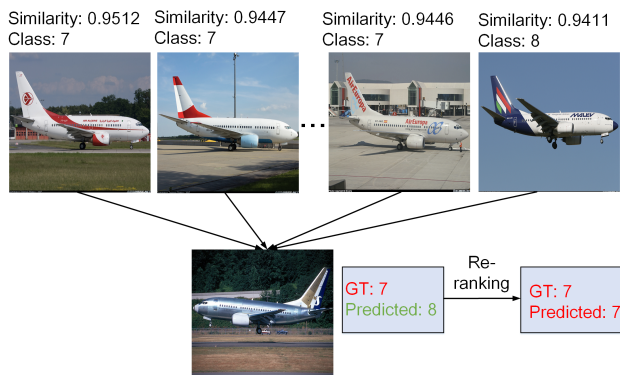


Figure 5. Rectifying a misclassified image by re-ranking. The ground-truth of the testing image is class 7, and it is misclassified into class 8 by a low classification probability. The *topn* images with the highest similarity scores are retrieved from the database, and an new re-ranked score is calculated for each of the *topn* classes according to Equation 8. Finally, the class 7 with the biggest re-ranked score is taken as the recognized class.

and Airs). More analysis about these re-ranking parameters is given in the ablation experiments.

4.3. Quantitative Analysis

We compare our CCFR with a number of recent works on three widely used benchmarks in Table 2. From the results, we find that our method outperforms all previous methods. To conduct fair comparisons with existing mod-

els, we use ResNet-50 as the feature extractor which is commonly used. Given that object/part annotations are labor-intensive or infeasible in practice, we train our CCFR with only image-level labels.

The third column of Table 2 shows the comparison results on CUB-200-2011. It shows that our CCFR achieves the highest Top1 accuracy and increases the accuracy by 0.7%. Compared to NTS[38] which tries to obtain informative local regions with a ranking loss, we utilize the triplet loss to select more discriminative local regions, leading to better attention on discriminative areas such as bird’s head, wings and feet as shown in Fig 4. Comparing with StackLSTM[12] which is the best result in CUB-200-2011 up to now, we achieve a 0.7% improvement. Besides, it is worth noting that StackLSTM is a very messy multi-stage training model that hampers the availability in practical use, while our proposed CCFR is easier to implement.

The fourth and fifth columns show the comparison results on Stanford Cars and FGVC Aircraft respectively. Our CCFR achieves new state-of-the-art results with 94.1% Top1 accuracy on FGVC Aircraft and 95.49% Top1 accuracy on Stanford Cars. In the second last row of Table 2, we show that our CCFR w\o re-ranking also achieves satisfactory results which benefit from the elaborately designed architecture and effective training loss (i.e. the triplet loss for local regions, and the Multi-level loss for pretraining).

Also, from the last two rows, it is clear that re-ranking can bring further improvement for the Top1 accuracy (especially when the Top1 softmax probability is relatively low,

Model	Multi-level loss	Scale-separated NMS	Fusion Network	Re-ranking	CUB Acc.(%)
ResNet-50					84.5
ResNet-50	✓				85.2
ResNet-50 + local region	✓				90.3
ResNet-50 + local region	✓	✓			90.4
ResNet-50 + local region	✓	✓	✓		90.7
CCFR	✓	✓	✓	✓	91.1

Table 3. Ablation experiments for investigating the influence of different components about our method on CUB. The columns represent the different components (Multi-level loss, Scale-separated NMS, Fusion Network and Re-ranking). The rows represent the different models, where "ResNet-50 + local region" means that local regions are utilized in addition to the global features, and CCFR is our proposed method.

Method	CUB	Airs	Cars
Retrieval	88.8	93.4	91.54
Classification	90.7	93.1	95.37
CCFR	91.1	94.1	95.49

Table 4. The comparison of the accuracy among Retrieval, Classification and CCFR on different datasets.

which usually means the model hesitates among the $topn$ classes). By re-ranking the $topn$ classes with the statistic of the $topm$ ($topm=50$) most similar retrievals from the database (usually constructed with the training samples), we probably rectify the uncertain Top1 class and rank the more confident class to Top1, and thus increase the Top1 accuracy (see Equation 8). Fig 5 shows the misclassified image is rectified by re-ranking. Specifically, the ground-truth of the testing image is class 7 which is misclassified into class 8 by a low Softmax probability. Then we select the $topm$ images with the highest similarity scores from the database, and get a new score for each of the $topn$ classes according to our formulation, and finally take the class (class 7) with the biggest new score as the recognized class.

4.4. Ablation Experiments

To investigate the influence of different components of our CCFR architecture, we conduct ablation studies and report the results.

Influence of Multi-level Loss. We investigate the influence of our Multi-level loss through experiments with standard Softmax loss. As shown in the second and third rows of Table 3, by applying our designed Multi-level loss on ResNet-50, the Top1 accuracy is improved by 0.7%, which demonstrates its effectiveness. In this work, we utilize the Multi-level loss to pretrain the ResNet-50 as initialization of the backbone of our CCFR for better performance.

Influence of Scale-separated NMS. As shown in the fourth and fifth rows of Table 3, by applying the Scale-separated NMS, the performance improves from 90.3% to 90.4%, where the fourth row conducts the conventional NMS on all boxes collected from different scales, and the fifth row adopts the scale-separated NMS to reduce the mu-

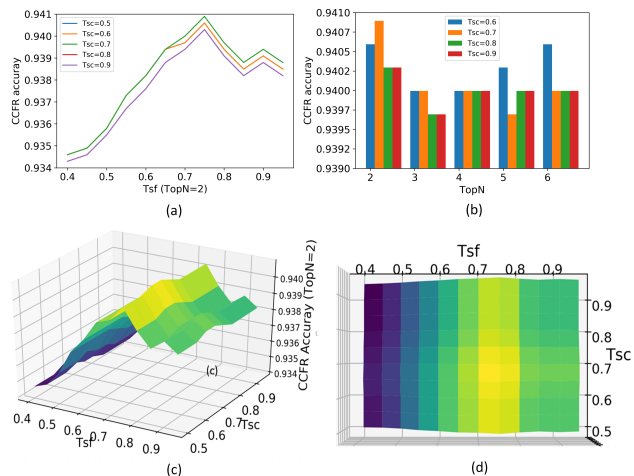


Figure 6. Ablation experiments for the main re-ranking parameters on FGVC Aircraft. Sub-figure (a) shows the influence of different T_{sf} and T_{sc} values ($topn$ is fixed to 2). Sub-figure (b) shows the impact of different $topn$ and T_{sc} values while fixing T_{sf} to 0.75. Sub-figure (c) and (d) visualize the surface over T_{sc} and T_{sf} respectively from different views, where warm color (yellow) means high accuracy and cold color (blue) represents low accuracy.

tual influence among different scale boxes. The results verify the effectiveness of the Scale-separated NMS.

Influence of Fusion Network. From the comparison between the fifth and the sixth rows in Table 3, we can find that the Top1 accuracy is improved from 90.4% to 90.7%, where the sixth row adopts Fusion Network (describe in section 3.2) to fuse the local region features obtaining from scale-separated NMS, while the fifth row directly concatenates these features after the global average pooling.

Influence of Re-ranking. Since our CCFR is a retrieval-based model, we also compare the results obtained only by retrieval in Table 4. Specifically, we first compute the cosine similarity between the testing image and all the training images in database, and then use the Top1 image label as the final result. We can find that classification-based results are much better than retrieval-based results on CUB-

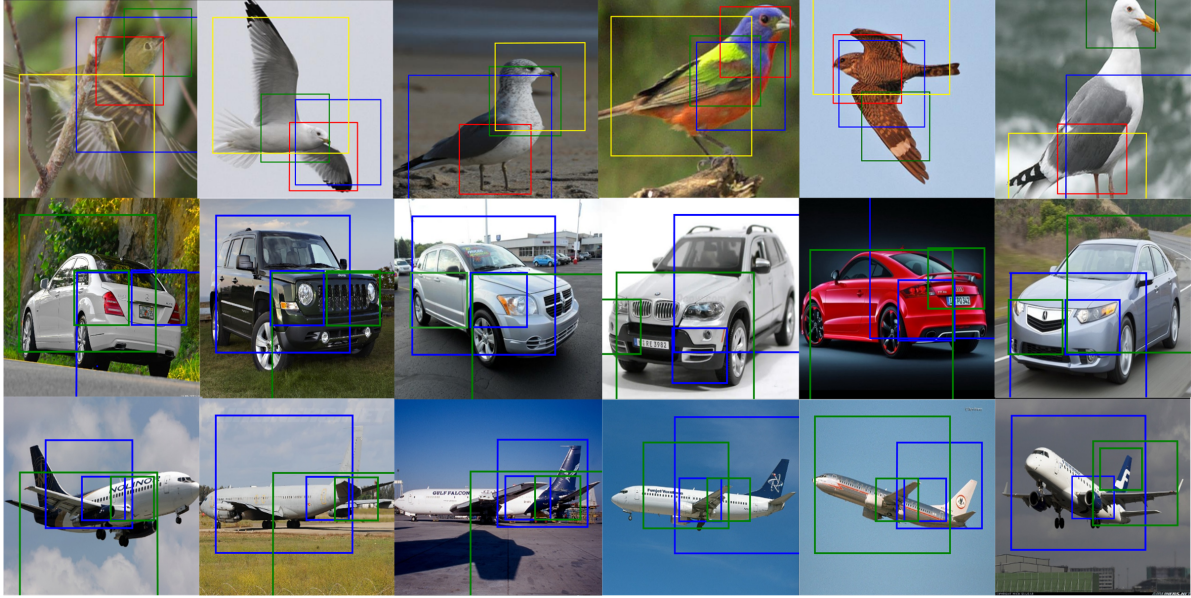


Figure 7. Illustration of the Top4 selected boxes by our model on three benchmark datasets. The bird’s head and wings are deemed as the most crucial areas for birds, and for the cars are the light and head/tail, and for the airs are the turbine and tail.

200-2011 and Stanford Cars (competitive on the FGVC Aircraft). And the last row in Table 4 verifies the idea that the combination of the retrieval and the classification can bring performance improvement. To further investigate the influence of the main re-ranking parameters, i.e. T_{sf} , T_{sc} and $topn$ as described in Equation 8, more ablation experiments are conducted on the FGVC Aircraft dataset. Specifically, we investigate the change of the CCFR accuracy by ranging $topn$ from 2 to 6, T_{sf} from 0.4 to 0.95, and T_{sc} from 0.5 to 0.95 (Note that $topm$ is completely determined by T_{sc} , α and β are simply set to 0 and 1.0). All the results as shown in Fig 6. From Fig 6 (a), we can find that for different T_{sc} , the curves have the same trend and CCFR accuracy achieves the highest value when T_{sc} is 0.7 and T_{sf} is 0.75 (here $topn$ is fixed to 2, and a consistent phenomenon can be observed for other $topn$ values). In Fig 6 (b), we compare the effect of different T_{sc} and $topn$ values while fixing T_{sf} to 0.75 (the optimal value in (a)), and we can find the accuracy achieves best when T_{sc} is 0.7 and $topn$ is 2 (it seems that most misclassified cases occur between the first and second place ranked by the Softmax probabilities). With $topn$ fixed to 2, Fig 6 (c) (d) visualize the surface of the CCFR accuracy over T_{sc} and T_{sf} respectively from different views, where warm color (yellow) represents high accuracy and cold color (blue) represents low accuracy. It can be clearly see that, T_{sf} has the greatest influence on the re-ranking effect (which is reasonable), and the accuracy is insensitive to T_{sc} (which means a wide range of T_{sc} could achieve similar accuracy).

4.5. Qualitative Analysis

We draw the selected boxes in Fig 7 to better analyze the regions where our model focuses on. Two boxes with the highest confidence score are shown for each scale. It can be seen that, except for the region containing the whole object, our model deems head and wing as the most crucial areas for birds (the top two rows), and the light and head/tail for cars, and the turbine and tail for airs. All of these are consistent with human intuition.

5. Conclusion

In this work, we propose a Coarse Classification and Fine Re-ranking framework for the FGVC problem and get state-of-the-art results on three common datasets, where local region enhanced features are generated to re-rank the $topn$ classification results predicted by the semantic global features. We design an effective structure to integrate the local and global features, and use the triplet loss to discover more discriminative regions for distinguishing hard samples (supervised with only image-level labels). And to learn more effective semantic global features, we design a Multi-level loss acted on an auto-clustered hierarchical category structure for the backbone network pretraining. Some ablation experiments are provided for further analysis, which makes the work more convinced and solid.

References

- [1] Archith John Bency, Heesung Kwon, Hyungtae Lee, S. Karthikeyan, and B. S. Manjunath. Weakly supervised local-

- ization using deep feature maps. In *ECCV*, pages 714–731, 2016. 2
- [2] T. Berg and P. Belhumeur. Poof: Part-based one-vs.-one features for fine-grained categorization, face verification, and attribute estimation. *2013 IEEE Conference on Computer Vision and Pattern Recognition*, pages 955–962, 2013. 2
- [3] Steve Branson, Grant Van Horn, Serge J. Belongie, and Pietro Perona. Bird species categorization using pose normalized deep convolutional nets. *CoRR*, abs/1406.2952, 2014. 2
- [4] Bingyi Cao, Andre Araujo, and Jack Sim. Unifying deep local and global features for efficient image search. *CoRR*, abs/2001.05027, 2020. 1, 2
- [5] Yuning Chai, Victor Lempitsky, and Andrew Zisserman. Symbiotic segmentation and part localization for fine-grained categorization. In *Proceedings of the IEEE International Conference on Computer Vision*, pages 321–328, 2013. 2
- [6] Yue Chen, Yalong Bai, Wei Zhang, and Tao Mei. Destruction and construction learning for fine-grained image recognition. In *Proceedings of the IEEE Conference on Computer Vision and Pattern Recognition*, pages 5157–5166, 2019. 6
- [7] Yin Cui, Yang Song, Chen Sun, Andrew Howard, and Serge Belongie. Large scale fine-grained categorization and domain-specific transfer learning. In *Proceedings of the IEEE conference on computer vision and pattern recognition*, pages 4109–4118, 2018. 1, 2, 3, 6
- [8] Jia Deng, Wei Dong, Richard Socher, Li-Jia Li, Kai Li, and Li Fei-Fei. Imagenet: A large-scale hierarchical image database. In *2009 IEEE conference on computer vision and pattern recognition*, pages 248–255. Ieee, 2009. 2
- [9] Ruoyi Du, Dongliang Chang, Ayan Kumar Bhunia, Jiyang Xie, Yi-Zhe Song, Zhanyu Ma, and Jun Guo. Fine-grained visual classification via progressive multi-granularity training of jigsaw patches. In *European Conference on Computer Vision*, 2020. 1, 2, 3, 6
- [10] Abhimanyu Dubey, Otkrist Gupta, Pei Guo, Ramesh Raskar, Ryan Farrell, and Nikhil Naik. Pairwise confusion for fine-grained visual classification. In *The European Conference on Computer Vision (ECCV)*, September 2018. 6
- [11] Efstratios Gavves, Basura Fernando, Cees GM Snoek, Arnold WM Smeulders, and Tinne Tuytelaars. Fine-grained categorization by alignments. In *Proceedings of the IEEE international conference on computer vision*, pages 1713–1720, 2013. 2
- [12] Weifeng Ge, Xiangru Lin, and Yizhou Yu. Weakly supervised complementary parts models for fine-grained image classification from the bottom up. In *CVPR*, pages 3034–3043, 2019. 1, 2, 3, 6
- [13] Xiangteng He, Yuxin Peng, and Junjie Zhao. Which and how many regions to gaze: Focus discriminative regions for fine-grained visual categorization. *International Journal of Computer Vision*, 127(9):1235–1255, 2019. 2
- [14] Ruyi Ji, Longyin Wen, Libo Zhang, Dawei Du, Yanjun Wu, Chen Zhao, Xianglong Liu, and Feiyue Huang. Attention convolutional binary neural tree for fine-grained visual categorization. In *Proceedings of the IEEE/CVF Conference on Computer Vision and Pattern Recognition*, pages 10468–10477, 2020. 6
- [15] Dahun Kim, Donghyeon Cho, and Donggeun Yoo. Two-phase learning for weakly supervised object localization. In *ICCV*, pages 3554–3563, 2017. 2
- [16] Dimitri Korsch, Paul Bodesheim, and Joachim Denzler. Classification-specific parts for improving fine-grained visual categorization. In *German Conference on Pattern Recognition*, pages 62–75. Springer, 2019. 1, 2, 3, 6
- [17] Dimitri Korsch, Paul Bodesheim, and Joachim Denzler. End-to-end learning of a fisher vector encoding for part features in fine-grained recognition. *CoRR*, abs/2007.02080, 2020. 2
- [18] Jonathan Krause, Benjamin Sapp, Andrew Howard, Howard Zhou, Alexander Toshev, Tom Duerig, James Philbin, and Li Fei-Fei. The unreasonable effectiveness of noisy data for fine-grained recognition. In *ECCV*, pages 301–320, 2016. 2
- [19] Jonathan Krause, Michael Stark, Jia Deng, and Li Fei-Fei. 3d object representations for fine-grained categorization. In *Proceedings of the IEEE international conference on computer vision workshops*, pages 554–561, 2013. 1, 5
- [20] Hao Li, Xiaopeng Zhang, Hongkai Xiong, and Qi Tian. Attribute mix: Semantic data augmentation for fine grained recognition. *CoRR*, abs/2004.02684, 2020. 1, 2, 3, 6
- [21] Zhichao Li, Yi Yang, Xiao Liu, Feng Zhou, Shilei Wen, and Wei Xu. Dynamic computational time for visual attention. In *Proceedings of the IEEE International Conference on Computer Vision Workshops*, pages 1199–1209, 2017. 1, 2, 3, 6
- [22] Di Lin, Xiaoyong Shen, Cewu Lu, and Jiaya Jia. Deep LAC: deep localization, alignment and classification for fine-grained recognition. In *CVPR*, pages 1666–1674, 2015. 2
- [23] Tsung-Yu Lin, Aruni RoyChowdhury, and Subhransu Maji. Bilinear CNN models for fine-grained visual recognition. In *ICCV*, pages 1449–1457, 2015. 2
- [24] Tsung-Yi Lin, Piotr Dollár, Ross Girshick, Kaiming He, Bharath Hariharan, and Serge Belongie. Feature pyramid networks for object detection. In *Proceedings of the IEEE conference on computer vision and pattern recognition*, pages 2117–2125, 2017. 2, 4
- [25] Jiongxin Liu, Angjoo Kanazawa, David Jacobs, and Peter Belhumeur. Dog breed classification using part localization. In *European conference on computer vision*, pages 172–185. Springer, 2012. 2
- [26] Subhransu Maji, Esa Rahtu, Juho Kannala, Matthew Blaschko, and Andrea Vedaldi. Fine-grained visual classification of aircraft. *arXiv preprint arXiv:1306.5151*, 2013. 1, 5
- [27] Maxime Oquab, Léon Bottou, Ivan Laptev, and Josef Sivic. Is object localization for free? - weakly-supervised learning with convolutional neural networks. In *CVPR*, pages 685–694, 2015. 2
- [28] Florian Schroff, Dmitry Kalenichenko, and James Philbin. Facenet: A unified embedding for face recognition and clustering. In *Proceedings of the IEEE conference on computer vision and pattern recognition*, pages 815–823, 2015. 2, 4
- [29] Marcel Simon, Yang Gao, Trevor Darrell, Joachim Denzler, and Erik Rodner. Generalized orderless pooling performs

- implicit salient matching. In *ICCV*, pages 4970–4979, 2017. [2](#)
- [30] Marcel Simon, Erik Rodner, Trevor Darrell, and Joachim Denzler. The whole is more than its parts? from explicit to implicit pose normalization. *IEEE Trans. Pattern Anal. Mach. Intell.*, pages 749–763, 2020. [1](#), [2](#), [3](#), [6](#)
- [31] Krishna Kumar Singh and Yong Jae Lee. Hide-and-seek: Forcing a network to be meticulous for weakly-supervised object and action localization. In *ICCV*, pages 3544–3553, 2017. [2](#)
- [32] Grant Van Horn, Steve Branson, Ryan Farrell, Scott Haber, Jessie Barry, Panos Ipeirotis, Pietro Perona, and Serge Belongie. Building a bird recognition app and large scale dataset with citizen scientists: The fine print in fine-grained dataset collection. In *Proceedings of the IEEE Conference on Computer Vision and Pattern Recognition*, pages 595–604, 2015. [2](#)
- [33] Catherine Wah, Steve Branson, Peter Welinder, Pietro Perona, and Serge Belongie. The caltech-ucsd birds-200-2011 dataset. 2011. [1](#), [5](#)
- [34] Zhuhui Wang, Shijie Wang, Haojie Li, Zhi Dou, and Jianjun Li. Graph-propagation based correlation learning for weakly supervised fine-grained image classification. In *The Thirty-Fourth AAAI Conference on Artificial Intelligence, AAAI 2020, The Thirty-Second Innovative Applications of Artificial Intelligence Conference, IAAI 2020, The Tenth AAAI Symposium on Educational Advances in Artificial Intelligence, EAAI 2020, New York, NY, USA, February 7-12, 2020*, pages 12289–12296. AAAI Press, 2020. [6](#)
- [35] Zhihui Wang, Shijie Wang, Shuhui Yang, Haojie Li, Jianjun Li, and Zezhou Li. Weakly supervised fine-grained image classification via gaussian mixture model oriented discriminative learning. In *CVPR*, pages 9746–9755, 2020. [2](#), [6](#)
- [36] Lin Wu, Yang Wang, Xue Li, and Junbin Gao. Deep attention-based spatially recursive networks for fine-grained visual recognition. *IEEE transactions on cybernetics*, 49(5):1791–1802, 2018. [6](#)
- [37] Lingxi Xie, Qi Tian, Richang Hong, Shuicheng Yan, and Bo Zhang. Hierarchical part matching for fine-grained visual categorization. In *Proceedings of the IEEE International Conference on Computer Vision*, pages 1641–1648, 2013. [2](#)
- [38] Ze Yang, Tiange Luo, Dong Wang, Zhiqiang Hu, Jun Gao, and Liwei Wang. Learning to navigate for fine-grained classification. In *ECCV*, pages 438–454, 2018. [1](#), [2](#), [3](#), [5](#), [6](#)
- [39] Lianbo Zhang, Shaoli Huang, Wei Liu, and Dacheng Tao. Learning a mixture of granularity-specific experts for fine-grained categorization. In *Proceedings of the IEEE International Conference on Computer Vision*, pages 8331–8340, 2019. [6](#)
- [40] Ning Zhang, Jeff Donahue, Ross B. Girshick, and Trevor Darrell. Part-based r-cnns for fine-grained category detection. In *ECCV*, pages 834–849, 2014. [2](#)
- [41] Ning Zhang, Evan Shelhamer, Yang Gao, and Trevor Darrell. Fine-grained pose prediction, normalization, and recognition. *CoRR*, abs/1511.07063, 2015. [2](#)
- [42] Xiaolin Zhang, Yunchao Wei, Jiashi Feng, Yi Yang, and Thomas S. Huang. Adversarial complementary learning for weakly supervised object localization. In *CVPR*, pages 1325–1334, 2018. [2](#)
- [43] Xiaopeng Zhang, Hongkai Xiong, Wengang Zhou, Weiyao Lin, and Qi Tian. Picking deep filter responses for fine-grained image recognition. In *CVPR*, pages 1134–1142, 2016. [2](#)
- [44] Heliang Zheng, Jianlong Fu, Tao Mei, and Jiebo Luo. Learning multi-attention convolutional neural network for fine-grained image recognition. In *ICCV*, pages 5219–5227, 2017. [6](#)
- [45] Heliang Zheng, Jianlong Fu, Zheng-Jun Zha, and Jiebo Luo. Learning deep bilinear transformation for fine-grained image representation. In *NeurIPS*, pages 4279–4288, 2019. [2](#)
- [46] Bolei Zhou, Aditya Khosla, Àgata Lapedriza, Aude Oliva, and Antonio Torralba. Learning deep features for discriminative localization. In *CVPR*, pages 2921–2929, 2016. [2](#)
- [47] Peiqin Zhuang, Yali Wang, and Yu Qiao. Learning attentive pairwise interaction for fine-grained classification. In *The Thirty-Fourth AAAI Conference on Artificial Intelligence, AAAI 2020, The Thirty-Second Innovative Applications of Artificial Intelligence Conference, IAAI 2020, The Tenth AAAI Symposium on Educational Advances in Artificial Intelligence, EAAI 2020, New York, NY, USA, February 7-12, 2020*, pages 13130–13137. AAAI Press, 2020. [1](#), [2](#), [3](#), [6](#)